El Niño-Southern Oscillation, the Madden-Julian Oscillation and Atlantic basin tropical cyclone rapid intensification

Philip J. Klotzbach[1]

Received 29 February 2012; revised 4 May 2012; accepted 7 June 2012; published 17 July 2012.

[1] Both El Niño-Southern Oscillation (ENSO) and the Madden-Julian Oscillation (MJO) have previously been documented to impact Atlantic basin tropical cyclone (TC) activity through alterations in large-scale fields such as vertical wind shear, mid-level moisture, sea level pressure and sea surface temperature. Atlantic TC activity has been shown to be enhanced when La Niña conditions are present in the tropical Pacific, while activity is reduced when El Niño conditions occur. Atlantic TC activity is enhanced when the convectively active phase of the MJO is over Africa and the western Indian Ocean (Phases 1–2), while TC activity is suppressed when the convectively active phase of the MJO is over the tropical Pacific (Phases 6–7). These relationships are shown to extend to Atlantic basin rapid intensification (RI) events (typically defined as intensification of 30 knots or greater in 24 h), with nearly three times as many RI events in La Niña years when compared with El Niño years. In addition, approximately four times more RI episodes occur when the MJO exceeds one standard deviation in Phases 1–2 than when the MJO exceeds one standard deviation in Phases 6–7. Storms forming in Phases 1–2 are twice as likely to undergo at least one RI episode during their lifetime as storms forming in Phases 6–7. Even stronger relationships are seen when the MJO and ENSO are considered in combination.

Citation: Klotzbach, P. J. (2012), El Niño-Southern Oscillation, the Madden-Julian Oscillation and Atlantic basin tropical cyclone rapid intensification, *J. Geophys. Res.*, *117*, D14104, doi:10.1029/2012JD017714.

1. Introduction

[2] El Niño-Southern Oscillation (ENSO) is a large-scale mode of coupled atmospheric/oceanic variability that impacts weather and climate around the globe [*Rasmusson and Carpenter*, 1982]. ENSO has significant impacts on tropical cyclone (TC) activity worldwide [*Camargo et al.*, 2007], with its notable impacts on seasonal Atlantic basin TC activity as well as U.S. hurricane landfalls being noted in a large number of studies [e.g., *Gray*, 1984; *Bove et al.*, 1998; *Klotzbach*, 2011]. While relationships have been documented for ENSO's impacts on basinwide activity levels around the globe, limited studies have been conducted into relationships between ENSO and rapid intensification (RI) of TCs (typically defined as an increase of 30 knots over a 24-h period [*Kaplan and DeMaria*, 2003]). *Wang and Zhou* [2008] documented that RI occurred more frequently in the Northwest Pacific in El Niño years (53% of TCs) compared with La Niña years (37% of TCs). The author is unaware of any studies that explicitly documented the impact of ENSO on Atlantic basin RI.

[3] The Madden-Julian Oscillation (MJO) is a large-scale mode of tropical variability that propagates around the globe on an approximately 30–60-day timescale [*Madden and Julian*, 1972]. As it does, it alters large-scale fields such as vertical wind shear, sea level pressure (SLP), mid-level moisture and vertical motion that have been shown in previous research to impact TC activity around the globe [e.g., *Camargo et al.*, 2009]. Specifically, alterations in Atlantic basin activity have been documented, with *Maloney and Hartmann* [2000] focusing on the Gulf of Mexico, while *Klotzbach* [2010] and *Ventrice et al.* [2011] focused on the Main Development Region (MDR). *Klotzbach* [2010] showed that when the convectively active phase of the MJO was located over Africa or in the western Indian Ocean (Phases 1–2 of the Wheeler-Hendon (WH) index [*Wheeler and Hendon*, 2004]), Atlantic TC activity was enhanced. Specifically, when the MJO index was greater than one standard deviation (SD) in amplitude, over twice as many systems formed in the MDR and became hurricanes at some point during their lifetime than when the convectively active phase of the MJO was located over the tropical Pacific (Phases 6–7 of the WH index). Stronger relationships were found for systems becoming major hurricanes.

[4] Given that climate conditions appear more favorable for Atlantic basin storm formation in particular phases of the MJO and ENSO than in others, this study examines the possibility that these impacts extend to RI events as well. Section 2 describes the data utilized, while section 3 examines the impacts of ENSO on Atlantic basin RI. Section 4

[1]Department of Atmospheric Science, Colorado State University, Fort Collins, Colorado, USA.

Corresponding author: P. J. Klotzbach, Department of Atmospheric Science, Colorado State University, Fort Collins, CO 80523, USA. (philk@atmos.colostate.edu)

0148-0227/12/2012JD017714

Table 1. Classification of Years by ENSO Phase Based Upon the August-September-September-October-Averaged MEI Index[a]

El Niño	Neutral	La Niña
1976 (+0.99)	1979 (+0.70)	1974 (−0.83)
1977 (+0.91)	1980 (+0.24)	1975 (−1.94)
1982 (+1.91)	1981 (+0.14)	1988 (−1.47)
1986 (+1.08)	1983 (+0.21)	1995 (−0.48)
1987 (+1.72)	1984 (−0.03)	1996 (−0.44)
1993 (+1.02)	1985 (−0.34)	1998 (−0.76)
1994 (+1.16)	1989 (−0.30)	1999 (−1.01)
1997 (+2.68)	1990 (+0.31)	2007 (−1.16)
2002 (+0.88)	1991 (+0.87)	2008 (−0.72)
2009 (+0.89)	1992 (+0.59)	2010 (−1.99)
	2000 (−0.32)	
	2001 (−0.20)	
	2003 (+0.47)	
	2004 (+0.49)	
	2005 (+0.04)	
	2006 (+0.84)	

[a]Average MEI values are provided in parentheses.

re-examines how large-scale fields in the MDR are modulated by the MJO, while section 5 examines how RI frequency changes with MJO phase. Section 6 examines how large-scale fields in the MDR are modulated by a combined MJO/ENSO index, while the strength of the relationship between RI and the combined MJO/ENSO index is considered in section 7. Section 8 concludes the manuscript and provides ideas for future work.

2. Data

[5] The Multivariate ENSO Index (MEI) was utilized to classify ENSO events [*Wolter and Timlin*, 1998]. The MEI uses a set of six atmospheric/oceanic predictors (sea level pressure, zonal and meridional surface wind, sea surface temperature (SST), surface air temperature and total cloud fraction) to define ENSO and is generally considered to be a more robust metric of ENSO than simply using an SST index such as Nino 3.4. The MEI index is calculated using a bi-monthly average (e.g., August–September). For the Atlantic hurricane season, the average of the August–September and September–October MEI values are utilized. The ten highest values of the index since 1974 are classified as El Niño, the ten lowest values are classified as La Niña while the sixteen years in the middle are classified as neutral. All years since 1974 (excluding 1978) are utilized in this analysis, since this is when the MJO index is available in real-time. Table 1 displays the years classified as El Niño, neutral and La Niña using the MEI definition discussed above. Years in each column are listed in date order, with average August–September–September–October values listed in parentheses.

[6] The index utilized to classify the MJO was developed by *Wheeler and Hendon* [2004]. They employed a multivariate EOF technique to attempt to isolate the MJO signal utilizing upper- and lower-level winds and outgoing longwave radiation (OLR). They defined two Real-Time Multivariate MJO (RMM) modes utilizing these fields. This index removes the seasonal cycle as well as some of the variability at lower frequencies associated with ENSO. The WH index is available from 1974–present, with data missing from April–December 1978 when OLR was unavailable. For this study, the period from 1974 to 2010 (except 1978) was examined. The WH index is available in near real-time and was downloaded from the Centre for Australian Weather and Climate Research (CAWCR) website: http://cawcr.gov.au/staff/mwheeler/maproom/RMM/. Figure 1 displays 200-mb velocity potential anomalies for the 200 days where the MJO is of the strongest amplitude for each of the eight phases of the MJO as defined by the WH index. Negative velocity potentials (cool colors) denote areas of upper-level divergence where convection is enhanced, while positive velocity potentials (warm colors) indicate areas where convection is suppressed. When enhanced convection associated with the MJO is maximized in the Western Hemisphere and Africa and suppressed convection is maximized over the western tropical Pacific, the WH index is in Phases 8 and 1. Enhanced convection maximized over the Indian Ocean and suppressed convection maximized over the central and eastern tropical Pacific is associated with a WH index in Phases 2 and 3. When enhanced convection is maximized over the Maritime Continent and suppressed convection is maximized over the tropical Atlantic, the WH index is in Phases 4 and 5. When enhanced convection is maximized over the tropical Pacific and suppressed convection is maximized over Africa and the Indian Ocean, the WH index is in Phases 6 and 7.

[7] An additional index available on the CAWCR website is one that analyzes a similar tropical convective signal to that analyzed by the WH index but with ENSO and the 120-day-mean retained. This index is utilized to approximate the combined signal of the MJO and ENSO in this analysis and is referred to as the WH-Combined index throughout the remainder of this manuscript. All calculations for both the WH index and the WH-Combined index are done for systems where the index (RMM1 + RMM2) is greater than one (approximately 60% of days during the hurricane season). This helps to separate out periods during which the MJO is inactive.

[8] TC statistics were calculated from the NHC's Best Track file available online at http://www.nhc.noaa.gov/data/hurdat/tracks1851to2010_atl_reanal.txt. Rapid intensification (RI) events were defined when a system intensified by 25-, 30-, 35-, and 40 or more knots in a 24-h period. In order to avoid potential issues with tropical depression classifications, only RI events beginning when a system was at least of 35-knot strength were counted in this analysis.

[9] The National Centers for Environmental Prediction/National Center for Atmospheric Research (NCEP/NCAR) Reanalysis I [*Kistler et al.*, 2001] was utilized for all large-scale field calculations. Since no daily global SST data is available since 1974, the reanalysis-derived skin temperature was used as a proxy for SST. The skin temperature is referred to as SST throughout the manuscript. All large-scale fields are calculated over the Main Development Region (MDR), which is defined to be 7.5–22.5°N, 75–20°W for this analysis, in keeping with the definition utilized by *Klotzbach* [2010].

3. ENSO Impacts on Atlantic Basin RI

[10] ENSO's impacts on Atlantic basin TCs have been related to a variety of physical fields, including changes in vertical wind shear, mid-level moisture, upper-tropospheric

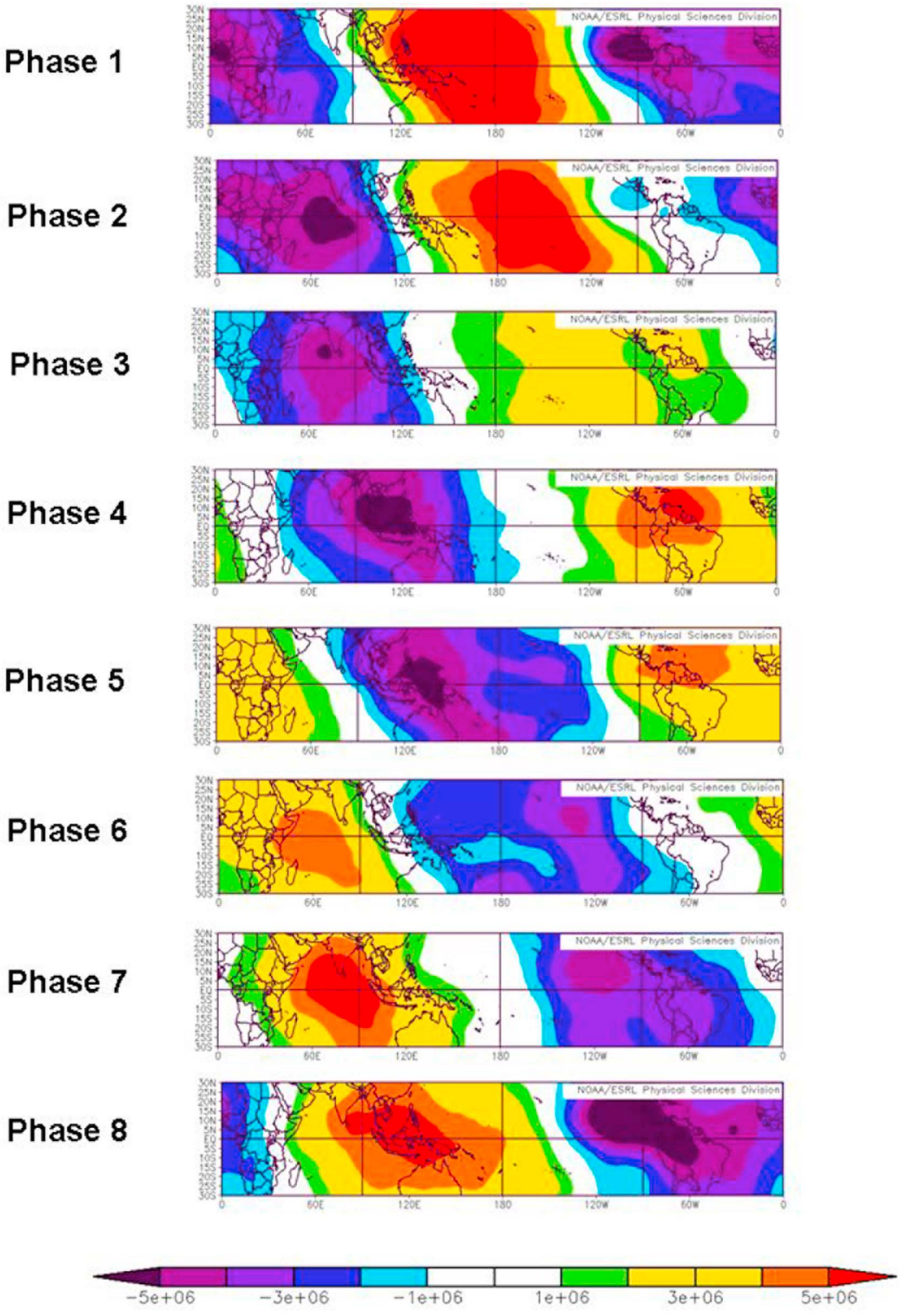

Figure 1. The 200-mb velocity potential anomalies ($m^2\ s^{-1}$) for the top 200 days for each MJO phase from July–October for each phase of the WH index. Cool colors indicate upper-level divergence while warm colors indicate upper-level convergence.

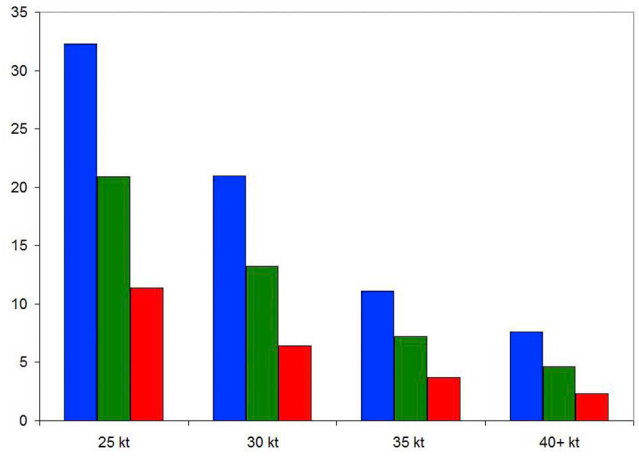

Figure 2. Average per-year 24-h periods for systems undergoing RI of 25-knot, 30-knot, 35-knot and 40+-knot thresholds for the entire Atlantic basin for years classified as La Niña (blue column), neutral (green column) and El Niño (red column). See text for ENSO classification scheme.

temperature and static stability [*Gray*, 1984; *Tang and Neelin*, 2004; *Klotzbach*, 2010]. In general El Niño is associated with fewer and weaker TCs in the Atlantic basin, especially in the Caribbean and Main Development Region, while La Niña is typically associated with more frequent and intense TCs in both of these areas [*Klotzbach*, 2010]. Given previous research, it is expected that Atlantic basin RI frequency might also be increased in La Niña years. Figure 2 displays the number of 24-h RI events for various categories (from 25 to 40+ knots in 24 h) for the entire Atlantic basin, while Figure 3 displays the same information but specifically for the MDR. Approximately three times as many RI events occurred in La Niña years compared with El Niño years when the entire Atlantic basin is examined. When only systems forming in the MDR are considered, the ratio differences between La Niña and El Niño grow considerably to approximately 6:1. Differences between La Niña and El Niño means for each RI threshold for the entire Atlantic basin as well as for the MDR-only are significant at the 1% level using a two-tailed Student's t-test and assuming that each year represents an individual degree of freedom.

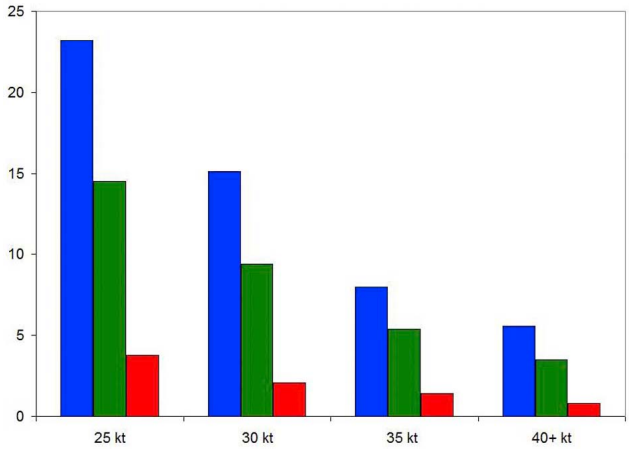

Figure 3. As in Figure 2 but for systems forming in the Atlantic MDR.

[11] Another way to evaluate ENSO's impacts on RI is to examine the frequency of storms intensifying by various RI thresholds given a particular phase of ENSO (Table 2). While differences are noted between El Niño and La Niña for all systems, the percentage differences are much stronger when only systems in the MDR are examined. For example, 32% of systems forming in the MDR in a La Niña year undergo at least one 40+ knot RI at some point during their lifetime, while only 12% of systems forming in the MDR in an El Niño year undergo this level of RI. Percentage differences between El Niño and La Niña at all four RI intensity thresholds examined in this study are statistically significantly different at the 5% level. Therefore, simply knowing the phase of ENSO provides a significant level of information regarding whether a system is likely to undergo RI.

4. MJO Impacts on Large-Scale Fields in the MDR

[12] *Klotzbach* [2010] calculated the impacts of the MJO on MDR large-scale fields in detail, and this paper briefly updates the analysis with an additional three years (2008–2010) of data. In addition, this paper investigates parameters over the July–October period instead of the June–November period examined in *Klotzbach* [2010]. This is due to the fact that only four out of 169 named storms that formed in the MDR did so outside of the months of July–October. Also, in order to remove periods when the MJO was considered to be weak, only MJO days that exceeded one SD were examined (approximately 60% of all days according to the WH definition).

[13] In a similar analysis to what was done in Table 1 of *Klotzbach* [2010], anomalies were next calculated and averaged over the MDR for July–October values for SST, SLP, 200-mb zonal wind (U), 850-mb U, 200–850-mb U shear, 700-mb relative humidity (RH), 300-mb omega and OLR when the MJO was greater than one SD for each phase of the MJO (Table 3). Differences between Phases 1+2 and Phases 6+7 are highlighted, as this is where the strongest differences were found in *Klotzbach* [2010]. These differences approach 5 ms^{-1} when averaged across the MDR for 200–850-mb U shear, implying a much more conducive environment for TC formation in Phases 1+2 than in Phases 6+7. When counting individual MJO events as one degree of freedom, differences significant at the 1% level

Table 2. Percentage Chance of All Atlantic Basin TCs and TCs Forming in the MDR in Each Phase of ENSO Having a RI Event of 25 Knots, 30 Knots, 35 Knots and 40+ Knots Over 24 h, Based on Data From 1974 to 2010 (Except 1978)

ENSO Phase	25 Kt	30 Kt	35 Kt	40+ Kt
		All TCs		
La Niña	53%	43%	29%	23%
Neutral	46%	36%	22%	14%
El Niño	39%	27%	17%	12%
		MDR TCs		
La Niña	67%	58%	39%	32%
Neutral	60%	50%	35%	23%
El Niño	36%	28%	20%	12%

Table 3. MDR-Averaged Anomalies for 200 mb U (ms^{-1}), 850 mb U (ms^{-1}), 200–850-mb U Shear (ms^{-1}), SST (°C), SLP (mb), 700 mb RH (%), 300 mb ω (mb d^{-1}) and OLR (W m^{-2})[a]

MJO Phase	Days per Phase	200- mb U	850- mb U	200–850 mb U	SST	SLP	700 mb RH	300 mb ω	OLR
1	446	−1.29	0.17	−1.46	−0.06	−0.44	0.74	−1.22	−1.51
2	398	−2.73	0.76	−3.48	0.10	−0.46	1.95	−1.98	−2.97
3	216	−1.93	0.33	−2.30	0.03	0.29	0.67	1.16	1.36
4	256	−0.02	0.27	−0.29	0.24	0.10	−0.13	1.92	2.07
5	456	1.07	−0.13	1.20	0.09	0.24	0.15	0.09	1.12
6	311	1.23	−0.61	1.84	−0.10	0.41	−1.35	0.82	1.56
7	199	2.19	−0.79	2.98	−0.25	0.31	−1.52	−0.73	−0.46
8	224	1.51	0.00	1.51	−0.04	−0.46	−0.52	−0.08	−1.16
Phases 1+2		−2.01	0.46	−2.47	0.02	−0.45	1.35	−1.60	−2.24
Phases 6+7		1.71	−0.70	2.41	−0.18	0.36	−1.43	0.05	0.55
Phases 1+2 – Phases 6+7		**−3.72**	**1.16**	**−4.88**	*0.20*	**−0.81**	**2.78**	−1.65	−2.79

[a]Anomalies are calculated from July 1–October 31 for all days when the MJO has a magnitude greater than one standard deviation. Differences between Phases 1+2 and Phases 6+7 that are significant at the 5% level are highlighted in italics, while differences significant at the 1% level are highlighted in bold.

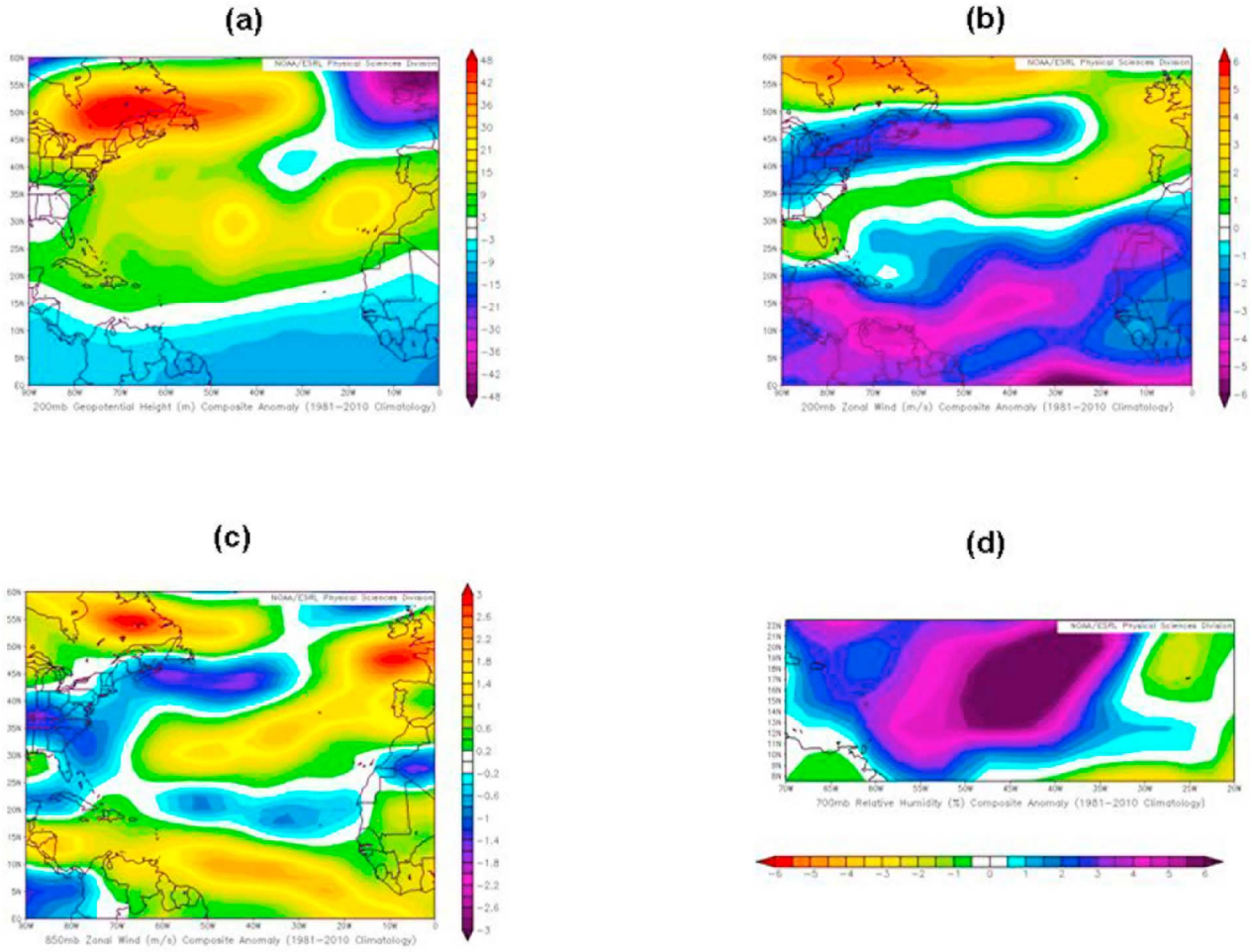

Figure 4. Difference between the 200 days with the highest amplitude in MJO Phase 2 during July–October minus the 200 days with the highest amplitude in MJO Phase 8 for (a) 200-mb height, (b) 200-mb zonal wind, (c) 850-mb zonal wind, and (d) 700-mb relative humidity. While Figures 4a–4c span most of the Atlantic, Figure 4d is focused on the MDR, as the relative humidity signal is very noisy outside of the MDR.

Table 4. Number of 24-h Periods for Systems Undergoing RI of 25-Knot, 30-Knot, 35-Knot and 40+-Knot Thresholds for All TCs in the Atlantic As Well As for Systems Forming in the MDR[a]

	24 Hour Periods				Normalized Values			
MJO Phase	25 Kt	30 Kt	35 Kt	40+ Kt	25 Kt	30 Kt	35 Kt	40+ Kt
				All Systems				
1	127	76	40	30	20.2	12.1	6.4	4.8
2	120	78	50	34	20.5	13.3	8.5	5.8
3	27	14	7	4	7.3	3.8	1.9	1.1
4	51	31	12	7	12.0	7.3	2.8	1.7
5	60	42	20	17	9.7	6.8	3.2	2.8
6	31	17	9	5	6.1	3.4	1.8	1.0
7	17	12	7	4	5.3	3.8	2.2	1.3
8	25	18	11	5	6.7	4.9	3.0	1.3
Phases 1+2/ Phases 6+7					3.5	3.7	3.9	4.9
				MDR Systems				
1	98	61	36	27	22.0	13.7	8.1	6.1
2	89	58	37	27	22.4	14.6	9.3	6.8
3	15	6	3	2	6.9	2.8	1.4	0.9
4	37	23	11	7	14.5	9.0	4.3	2.7
5	31	22	11	8	6.8	4.8	2.4	1.8
6	21	12	6	2	6.8	3.9	1.9	0.6
7	3	1	1	0	1.5	0.5	0.5	0.0
8	13	10	5	2	5.8	4.5	2.2	0.9
Phases 1+2/ Phases 6+7					5.4	6.3	7.2	18.6

[a]Also provided are values normalized by the number of days that the MJO spends in each phase for June–November for all TCs and for July–October for systems forming in the MDR. These normalized values are multiplied by 100, so they can be interpreted as the number of 24-h periods that one should expect given 100 days in a particular MJO phase. Ratios between Phases 1+2 and Phases 6+7 are provided for the normalized values.

are seen for all U quantities, SLP and 700-mb RH. Differences are significant at the 5% level for SST, while other differences are not statistically significant. All significance calculations are made using a two-tailed Student's t-test. Overall, the differences between phases are similar to what was found in *Klotzbach* [2010]. The findings of significant differences in 700-mb RH are similar to those found in *Camargo et al.* [2009], while the vertical shear changes noted here are much greater than those found in *Camargo et al.* [2009]. Differences in vertical shear and lower-to-mid level RH have been noted in previous work to impact RI frequency [*Kaplan and DeMaria*, 2003].

[14] One intriguing question based on these results is why the MDR is more conducive for TC formation in Phases 1+2 than in Phase 8, when the upper-level velocity potential anomalies appear most conducive (Figure 1). The primary reason seems to be in the reduction of vertical wind shear that occurs following the maximized velocity potential. When convection is enhanced over Africa and the western Indian Ocean, anomalous convergence associated with this enhancement implies lower-level westerly anomalies and upper-level easterly anomalies across the tropical Atlantic, both of which reduce vertical wind shear. Also, mid-level moisture is enhanced following the deep convective maximum. Figure 4 is a four-panel display showing how upper-level heights change from the 200 days with the highest amplitude in Phase 8 to the 200 days with the highest amplitude in Phase 2, with anomalous ridging in the subtropics and troughing near the equator in Phase 2 when compared with Phase 8 (Figure 4a). This height pattern produces anomalous easterlies at upper levels across the MDR (Figure 4b). Also changing from Phase 8 to Phase 2 are enhanced low-level westerlies (Figure 4c), which reduces the trade wind strength and consequently vertical wind shear. Enhancement of low-level moisture is also observed (Figure 4d). These factors in combination provide a more favorable dynamic and thermodynamic environment for TC formation, and as shown in the next section, RI as well.

5. MJO Impacts on Atlantic Basin RI

[15] Since predicting TC RI remains one of the great challenges in hurricane forecasting [*Sampson et al.*, 2011], the knowledge of RI likelihood given what phase of the MJO a particular storm forms in is likely to be useful to TC forecasters. While several studies have examined the impacts of the MJO on Atlantic basin TC activity, to the author's knowledge, no study has explicitly studied RI. All calculations displayed in the following paragraphs are done for systems when the MJO is greater than or equal to one SD. When the WH index is less than one SD, the MJO is likely not playing a significant role in altering tropical convection.

[16] As was done with ENSO, the relationships with the MJO are examined first for the entire Atlantic basin and then for the MDR. Stronger relationships are found between the MJO and systems forming in the MDR. Table 4 displays the number of 24-h periods for each RI threshold for all TCs in the Atlantic basin as well as just for systems forming in the MDR. Also provided are normalized values, given that the MJO, as defined by *Wheeler and Hendon* [2004], spends more time in some phases than in others. Normalized values for all TCs are calculated based upon the number of days the MJO spends in each phase from June–November, while normalized values for MDR TCs are calculated based upon the number of days that the MJO spends in each phase from July–October. This is due to the fact that virtually all TCs that form in the MDR do so from July–October. In addition, ratios between Phases 1+2 and Phases 6+7 are provided. All differences in the mean between Phases 1+2 and Phases 6+7 are statistically significant at the 1% level for systems forming in the MDR, assuming each coherent MJO event is one degree of freedom. While results for RI tend to be in line with overall TC activity results discussed in *Klotzbach* [2010], a drop in RI frequency is also noted for Phase 3,

Table 5. Percentage Chance of a Storm Forming in the MDR in Each Phase of the MJO Having a RI Event of 25 Knots, 30 Knots, 35 Knots and 40+ Knots, Based on Data From 1974 to 2010 (except 1978)[a]

MJO Phase	25 Kt	30 Kt	35 Kt	40+ Kt
1	84%	74%	53%	42%
2	69%	62%	42%	35%
3	56%	22%	11%	11%
4	62%	54%	38%	23%
5	47%	41%	29%	12%
6	38%	23%	23%	8%
7	20%	20%	20%	0%
8	40%	40%	40%	20%
Phase 1+2	76%	67%	47%	38%
Phase 6+7	33%	22%	22%	6%

[a]Also provided are the combined values for Phases 1+2 and Phases 6+7.

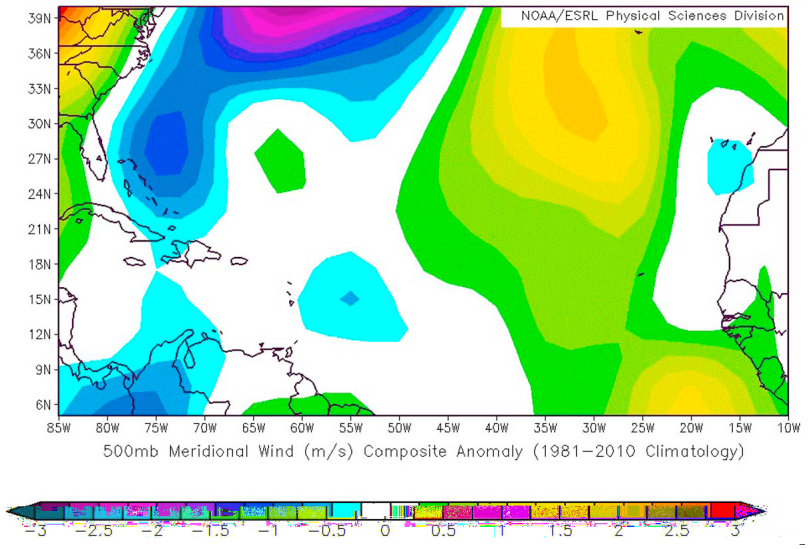

Figure 5. Difference between the 200 days with the highest amplitude in MJO Phases 1+2 during July–October minus the 200 days with the highest amplitude in MJO Phases 6+7 for 500-mb meridional wind. Small anomalies are observed west of 40°W in the MDR.

which generally has reasonably conducive overall conditions for TC genesis in the tropical Atlantic (Table 3). The reason for this drop in RI frequency in Phase 3 is the subject of current research.

[17] The normalized ratios between Phases 1+2 and Phases 6+7 especially stand out when examining RI periods for systems forming in the MDR. The ratio is greater than five to one for 24-h RI periods of 25 knots or more, while the ratio grows to greater than 18 to one for 24-h RI periods of 40 knot intensification or greater. Therefore, simply by knowing that a system forming in the MDR develops in a particular MJO phase (when the MJO is greater than one SD), gives some information about its likelihood for undergoing RI.

[18] Table 5 displays the odds for a system forming in the MDR for each phase of the MJO undergoing at least one RI episode during its lifetime. Large differences are seen between phases. For example, if a system forms in Phase 1 of the MJO, it has an 84% chance of undergoing at least one 25-knot RI episode during its lifetime; whereas if a system forms in Phase 7 of the MJO, it only has a 20% chance of undergoing at least one 25-knot RI. Similar strong relationships are found when examining more dramatic RI episodes of 40+ knots. For example, 42% of systems forming in the MDR in Phase 1 underwent at least one of these episodes, while no system forming in the MDR in Phase 7 over the period of record (1974–2010 except 1978) had an RI episode of this magnitude.

[19] The primary reason for the differences in RI frequency appear to be due to changes in environmental conditions as opposed to changes in formation location and large-scale steering flow. The average latitude-longitude formation point for TCs forming in the MDR in Phases 1+2 and in Phases 6+7 is virtually identical (approximately 15°N, 50°W). The 500-mb meridional wind shows very small differences between Phases 1+2 and Phases 6+7 west of 50°W in the MDR (Figure 5), indicating that the mid-level winds do not have more of a northerly component in Phases 1+2. If this were the case, it would tend to cause these TCs to stay in the MDR for a longer period of time.

6. MJO/ENSO Impacts on Large-Scale Fields in the MDR

[20] In order to evaluate the MJO and ENSO in combination, the WH index with ENSO and the 120-day mean retained is now considered. As is the case with the WH index with ENSO and the 120-day-mean removed, the WH-Combined index is divided into eight phases spanning the globe. Since the ENSO phase is retained in the WH-Combined index, certain phases of the index are preferentially experienced during the hurricane season in El Niño versus La Niña years. Table 6 displays the percentage of days that the WH-Combined index spends in each phase for El Niño, neutral and La Niña years, respectively during June–November. For example, Phases 7+8 (when tropical convective activity is enhanced in the western Pacific) occur in approximately 40% of hurricane season days when an El Niño is taking place, compared with only 5% of hurricane season days when a La Niña is occurring. Alternatively, Phases 2+3 (when tropical convective activity is enhanced in the tropical Indian Ocean) occur on approximately 47% of hurricane season days when La Niña is taking place,

Table 6. Percentage of Days That the WH-Combined Index Spends in Each Phase for El Niño Years, Neutral Years and La Niña Years During the Hurricane Season (June–November)

MJO Phase	El Niño	Neutral	La Niña
1	15%	14%	9%
2	7%	15%	24%
3	5%	12%	23%
4	5%	16%	21%
5	11%	15%	14%
6	17%	11%	6%
7	21%	8%	2%
8	20%	9%	3%

Table 7. MDR-Averaged Anomalies for 200 mb U (ms^{-1}), 850 mb U (ms^{-1}), 200–850-mb U Shear (ms^{-1}), SST (°C), SLP (mb), 700 mb RH (%), 300 mb ω (mb d^{-1}) and OLR (W m^{-2})[a]

MJO Phase	Days per Phase	200- mb U	850- mb U	200–850 mb U	SST	SLP	700 mb RH	300 mb ω	OLR
1	327	−1.60	0.09	−1.69	0.00	−0.25	0.49	−0.38	−0.86
2	484	−3.73	0.79	−4.53	0.08	−0.41	1.08	−1.69	−2.70
3	327	−2.49	0.60	−3.10	0.10	−0.19	0.75	−0.11	−0.06
4	370	0.80	−0.23	1.03	0.03	0.10	−0.36	−0.46	1.20
5	420	0.91	−0.29	1.20	−0.07	0.56	−1.06	2.18	3.47
6	347	1.18	−0.76	1.94	−0.13	0.55	−1.44	1.51	1.56
7	325	1.51	−0.55	2.06	−0.16	0.37	0.20	0.99	0.22
8	299	3.42	0.34	3.08	0.16	−0.73	0.34	−2.04	−2.83
Phases 2+3		−3.11	0.70	−3.81	0.09	−0.30	0.92	−0.90	−1.38
Phases 7+8		2.47	−0.10	2.57	0.00	−0.18	0.27	−0.52	−1.30
Phases 2+3 – Phases 7+8		**−5.58**	*0.80*	**−6.38**	0.09	−0.12	0.65	−0.37	−0.08

[a]Anomalies are calculated from July 1–October 31 for all days when the WH-Combined index has a magnitude greater than one standard deviation. Differences between Phases 2+3 and Phases 7+8 that are significant at the 5% level are highlighted in italics, while differences significant at the 1% level are highlighted in bold.

compared with only 12% of hurricane season days when El Niño is occurring.

[21] The next step involved calculating anomalies averaged over the MDR for July–October values for SST, SLP, 200-mb U, 850-mb U, 200–850-mb U shear, 700-mb RH, 300-mb omega and OLR when the WH-Combined index was greater than one SD (Table 7). Differences between Phases 2+3 and Phases 7+8 are highlighted, as this is where the strongest differences are typically found. The phase shift between the WH index and the WH-Combined index of one phase (e.g., the active phase is shifted from Phases 1+2 to Phases 2+3 while the inactive phase is shifted from Phases 6+7 to Phases 7+8) is likely due to the preferential state of La Niña associated with Phase 3 in the WH-Combined index and the preferential state of El Niño associated with Phase 8 in the WH-Combined index. Figure 6 displays the SST differences between the 200 days with the highest amplitude in Phase 3 for the WH-Combined index compared with the 200 days with the highest amplitude in Phase 3 for the WH index (Figure 6a). Figure 6b displays similar data for Phase 8. It is clearly seen that La Niña-like conditions are seen with Phase 3 of the WH-Combined index and El Niño-like conditions are seen with Phase 8 of the WH-Combined index. As was discussed earlier in this manuscript, cool ENSO conditions are much more conducive for Atlantic basin TC formation and RI.

[22] These differences are over 6 ms^{-1} when averaged across the MDR for 200–850-mb U shear, implying a much more conducive environment for TC formation in Phases 2–3 than in Phases 7–8. Differences for 200-mb U and 200–850-mb U are significant at the 1% level, while differences at the 850-mb U level are significant at the 5% level. Interestingly enough, differences are not statistically significant at the 5% level for any of the other dynamic or thermodynamic quantities examined in this analysis. Consequently, one can conclude that the WH-Combined indexes' power in determining RI frequency (documented in the next section) lies in its strong modulation of vertical shear. Figure 7 demonstrates the combined upward and downward-forced vertical motions associated with both the MJO (solid lines) and ENSO (dotted lines) for the WH-Combined index. Note that Phases 1 and 5 do not have arrows for ENSO, since neither El Niño or La Niña is strongly favored for those phases (Table 6). In general Phases 2–4 of the WH-Combined index are much more common in La Niña years, while Phases 6–8 are much more common in El Niño years.

7. Combined MJO/ENSO Impacts on Atlantic Basin RI

[23] As has been done with both ENSO and the WH index for the MJO by itself, the relationship with ENSO/MJO is examined first for the entire Atlantic basin and then for the MDR. Table 8 displays the number of 24-h periods for each RI threshold for all TCs in the Atlantic basin as well as just for systems forming in the MDR. As would be expected given the dramatic changes in vertical shear, the largest differences are observed between Phases 2+3 and Phases 7+8. All differences in the mean between Phases 2+3 and Phases 7+8 are statistically significant at the 1% level for systems forming in the MDR. The difference in means are somewhat greater when the WH-Combined index is considered compared with the WH index by itself, indicating that considering both the MJO and ENSO in combination can provide extra signal compared with either the MJO or ENSO by itself. The difference between Phases 2+3 and Phases 7+8 is emphasized when displaying tracks for all TCs undergoing a 30-knot or greater RI during 24 h (Figure 8).

[24] Table 9 displays the odds for a system forming in the MDR for each phase of the WH-Combined index undergoing at least one RI episode during its lifetime. Systems forming in Phases 2+3 have a 30-knot or greater 24-h RI episode 75% of the time, compared with only 17% of the time for systems forming in Phases 7+8. Consequently, simply knowing if the WH-Combined index is greater than one standard deviation on the day of TC formation provides a significant amount of information regarding its likelihood for having RI.

8. Summary and Future Work

[25] This paper showed the strong impact that both the MJO and ENSO have on RI episodes in the Atlantic basin. It began by examining ENSO's impacts on Atlantic basin RI and demonstrated that RI is much more frequent in La Niña events than in El Niño episodes with neutral ENSO events having RI frequency between cold and warm episodes. It

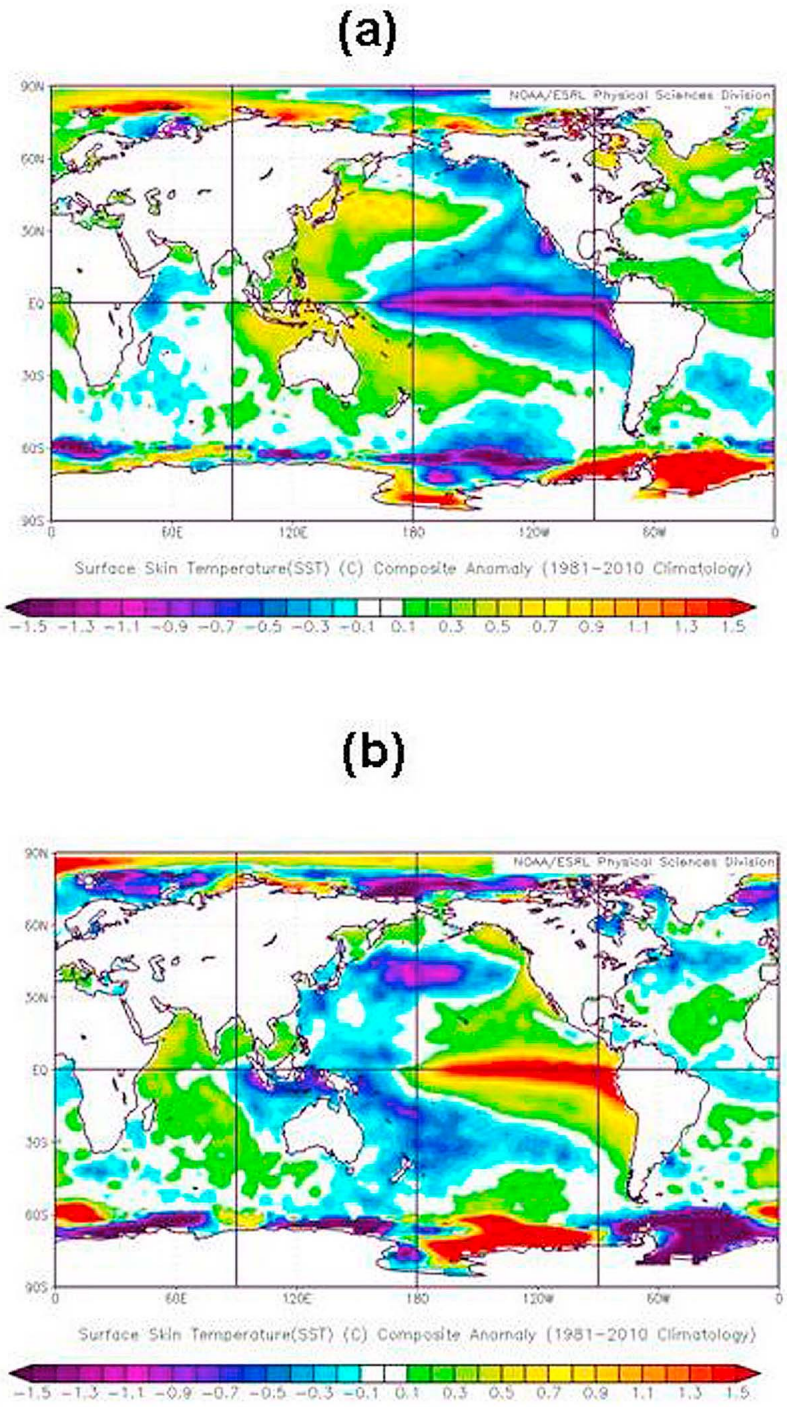

Figure 6. (a) Difference between the 200 days with the highest amplitude in Phase 3 for the WH-Combined index minus the 200 days with the highest amplitude in phase 3 for the WH index. (b) The same calculation for Phase 8 of the MJO.

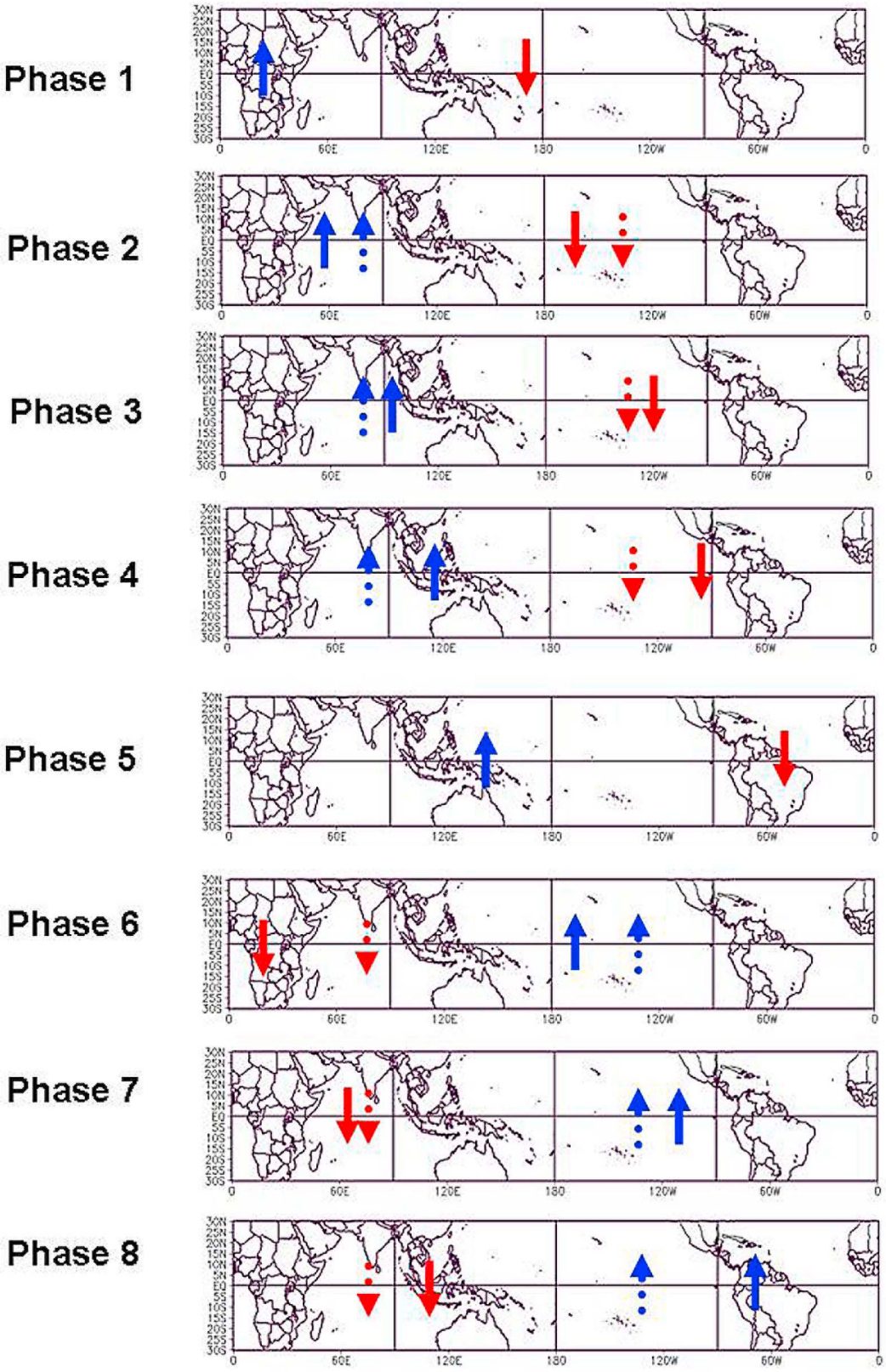

Figure 7. Anomalous vertical motion associated with the WH-Combined index. Solid lines represent anomalous vertical motion associated with the MJO, while dotted lines represent anomalous vertical motion associated with ENSO. Upward pointed arrows indicate anomalous ascent, while downward pointed arrows indicate anomalous descent.

Table 8. As in Table 4 but for the WH-Combined Index[a]

MJO Phase	24 Hour Periods				Normalized Values			
	25 Kt	30 Kt	35 Kt	40+ Kt	25 Kt	30 Kt	35 Kt	40+ Kt
				All Systems				
1	96	61	34	22	18.2	11.6	6.4	4.2
2	145	108	70	55	21.5	16.0	10.4	8.2
3	158	89	42	25	28.6	16.1	7.6	4.5
4	44	31	13	9	7.0	5.0	2.1	1.4
5	61	38	19	11	9.8	6.1	3.0	1.8
6	23	16	11	8	4.5	3.1	2.1	1.6
7	13	9	6	2	3.0	2.1	1.4	0.5
8	12	6	2	2	2.7	1.4	0.5	0.5
Phases 2+3/Phases 7+8					9.0	9.8	10.4	14.9
				MDR Systems				
1	68	43	25	17	20.8	13.1	7.6	5.2
2	117	84	53	43	24.2	17.4	11.0	8.9
3	117	70	31	19	35.8	21.4	9.5	5.8
4	17	12	7	5	4.6	3.2	1.9	1.4
5	34	24	14	9	8.1	5.7	3.3	2.1
6	12	6	3	0	3.5	1.7	0.9	0.0
7	0	0	0	0	0.0	0.0	0.0	0.0
8	6	3	0	0	2.0	1.0	0.0	0.0
Phases 2+3/Phases 7+8					29.0	38.2	INF	INF

[a]Ratios between Phases 2+3 and Phases 7+8 are provided for the normalized values.

then discussed the impact that the MJO has on large-scale conditions over the MDR. For example, conditions over the MDR are generally much more conducive for TC formation in the MDR in Phases 1+2 than it is in Phases 6+7. Given these relationships, RI episodes were then demonstrated to occur much more frequently in Phases 1+2 than in Phases 6+7, with other phases of the MJO showing relationships between these two extremes. When the MJO and ENSO were combined using the WH-Combined index, even stronger relationships were demonstrated.

[26] The most conducive phases for RI in the Atlantic MDR occur when deep convective anomalies occur over the tropical Indian Ocean. Associated with these deep convective anomalies in the Indian Ocean are increased mid-level moisture and reduced vertical wind shear in the tropical Atlantic, both of which are critical factors for RI. When deep convective anomalies are concentrated over the central and eastern tropical Pacific, the Atlantic MDR tends to be drier and have enhanced vertical wind shear, which reduces the likelihood of RI.

[27] One area of current research is determining whether incorporation of the daily MJO index would improve the skill of the Statistical Hurricane Intensity Prediction Scheme (SHIPS) [*DeMaria et al.*, 2005] or the recently developed

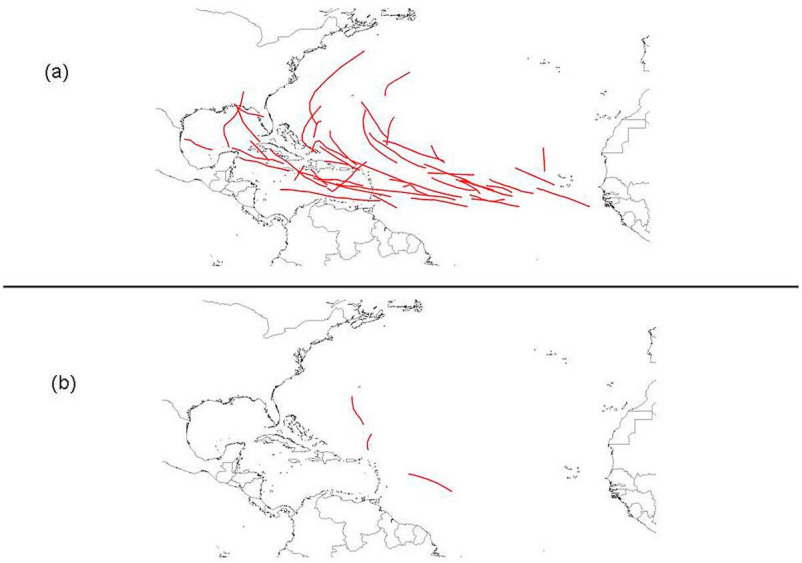

Figure 8. Tracks of TCs undergoing an RI of 30 knots or greater in 24 h during (a) Phases 2+3 defined by the WH-Combined index and (b) Phases 7+8 defined by the WH-Combined index. Normalized ratio differences between these phases is 38:1.

Table 9. As in Table 5 but for the WH-Combined Index

MJO Phase	25 Kt	30 Kt	35 Kt	40+ Kt
1	100%	77%	46%	38%
2	69%	66%	47%	47%
3	83%	71%	50%	33%
4	42%	33%	25%	17%
5	67%	53%	40%	20%
6	25%	17%	17%	0%
7	0%	0%	0%	0%
8	33%	33%	0%	0%
Phases 2+3	75%	68%	48%	41%
Phases 7+8	17%	17%	0%	0%

revised rapid intensity index [*Kaplan et al.*, 2010]. This statistical model typically provides the best real-time forecast guidance for the National Hurricane Center, and consequently, any improvements to the SHIPS model could help prevent loss of life and property. Additional avenues for research include examining other ways of combining the MJO and ENSO to maximize skill. The impact of the MJO and ENSO on RI in other global TC basins will also be investigated.

[28] **Acknowledgments.** Valuable discussions on the MJO and RI have been held with Eric Blake, Mark DeMaria, William Gray, John Knaff and Eric Maloney. The two anonymous reviewers are thanked for comments and suggestions that greatly improved the manuscript.

References

Bove, M. C., J. B. Elsner, C. W. Landsea, X. Niu, and J. J. O'Brien (1998), Effects of El Niño on U.S. landfalling hurricanes, revisited, *Bull. Am. Meteorol. Soc.*, *79*, 2477–2482, doi:10.1175/1520-0477(1998)079<2477:EOENOO>2.0.CO;2.

Camargo, S. J., K. A. Emanuel, and A. H. Sobel (2007), Use of a genesis potential index to diagnose ENSO effects on tropical cyclone genesis, *J. Clim.*, *20*, 4819–4834, doi:10.1175/JCLI4282.1.

Camargo, S. J., M. C. Wheeler, and A. H. Sobel (2009), Diagnosis of the MJO modulation of tropical cyclogenesis using an empirical index, *J. Atmos. Sci.*, *66*, 3061–3074, doi:10.1175/2009JAS3101.1.

DeMaria, M., M. Mainelli, L. K. Shay, J. A. Knaff, and J. Kaplan (2005), Further improvements to the Statistical Hurricane Intensity Prediction Scheme (SHIPS), *Weather Forecast.*, *20*, 531–543, doi:10.1175/WAF862.1.

Gray, W. M. (1984), Atlantic seasonal hurricane frequency. Part II: Forecasting its variability, *Mon. Weather Rev.*, *112*, 1669–1683.

Kaplan, J., and M. DeMaria (2003), Large-scale characteristics of rapidly intensification tropical cyclones in the North Atlantic basin, *Weather Forecast.*, *18*, 1093–1108, doi:10.1175/1520-0434(2003)018<1093:LCORIT>2.0.CO;2.

Kaplan, J., M. DeMaria, and J. A. Knaff (2010), A revised tropical cyclone rapid intensification index for the Atlantic and Eastern North Pacific basins, *Weather Forecast.*, *25*, 220–241, doi:10.1175/2009WAF2222280.1.

Kistler, R., et al. (2001), The NCEP-NCAR 50-year reanalysis: Monthly means CD-ROM and documentation, *Bull. Am. Meteorol. Soc.*, *82*, 247–267, doi:10.1175/1520-0477(2001)082<0247:TNNYRM>2.3.CO;2.

Klotzbach, P. J. (2010), On the Madden-Julian Oscillation–Atlantic hurricane relationship, *J. Clim.*, *23*, 282–293, doi:10.1175/2009JCLI2978.1.

Klotzbach, P. J. (2011), El Niño–Southern Oscillation's impacts on Atlantic basin hurricanes and U. S. landfalls, *J. Clim.*, *24*, 1252–1263, doi:10.1175/2010JCLI3799.1.

Madden, R. A., and P. R. Julian (1972), Description of global-scale circulation cells in the tropics with a 40–50 day period, *J. Atmos. Sci.*, *29*, 1109–1123, doi:10.1175/1520-0469(1972)029<1109:DOGSCC>2.0.CO;2.

Maloney, E. D., and D. L. Hartmann (2000), Modulation of hurricane activity in the Gulf of Mexico by the Madden-Julian Oscillation, *Science*, *287*, 2002–2004, doi:10.1126/science.287.5460.2002.

Rasmusson, E. M., and T. H. Carpenter (1982), Variations in tropical sea surface temperature and surface wind fields associated with the Southern Oscillation/El Niño, *Mon. Weather Rev.*, *110*, 354–384, doi:10.1175/1520-0493(1982)110<0354:VITSST>2.0.CO;2.

Sampson, C. R., J. Kaplan, J. Knaff, M. DeMaria, and C. Sisko (2011), A deterministic rapid intensification aid, *Weather Forecast.*, *26*, 579–585, doi:10.1175/WAF-D-10-05010.1.

Tang, B. H., and J. D. Neelin (2004), ENSO influence on Atlantic hurricanes via tropospheric warming, *Geophys. Res. Lett.*, *31*, L24204, doi:10.1029/2004GL021072.

Ventrice, M. J., C. D. Thorncroft, and P. E. Roundy (2011), The Madden-Julian Oscillation's influence on African easterly waves and downstream tropical cyclogenesis, *Mon. Weather Rev.*, *139*, 2704–2722, doi:10.1175/MWR-D-10-05028.1.

Wang, B., and X. Zhou (2008), Climate variation and prediction of rapid intensification in tropical cyclones in the western North Pacific, *Meteorol. Atmos. Phys.*, *99*, 1–16, doi:10.1007/s00703-006-0238-z.

Wheeler, M. C., and H. H. Hendon (2004), An all-season real-time multivariate MJO index: Development of an index for monitoring and prediction, *Mon. Weather Rev.*, *132*, 1917–1932, doi:10.1175/1520-0493(2004)132<1917:AARMMI>2.0.CO;2.

Wolter, K., and M. S. Timlin (1998), Measuring the strength of ENSO events—How does 1997/98 rank?, *Weather*, *53*, 315–324, doi:10.1002/j.1477-8696.1998.tb06408.x.